Development of a Subject-Specific CT-Based Finite Element Workflow for Regional Tibial Mechanical Assessment

Kiavash Sharifi[1], Alex Vadati[2], Ankur Padhye[3], John D. Willson[1], C. Ryan Steinbaker[4], Stacey A. Meardon[1]

[1]Department of Physical Therapy, East Carolina University, Greenville, NC, USA
[2]Department of Engineering, East Carolina University, Greenville, NC, USA
[3]Department of Physical Therapy, Idaho State University, Pocatello, ID, USA
[4]Eastern Radiologists, Greenville, NC, USA

INTRODUCTION: Bone stress injuries (BSIs) are common among athletes, and female athletes experience them two to four times more often than male athletes [1]. The tibia is the most frequently affected site, accounting for 33 to 55% of BSIs in athletic and military cohorts. Vulnerability varies along the length of the tibia: the distal third is most likely to develop injury and recurrence. Targeted prevention and treatment efforts, particularly for women, require clinical tools capable of assessing strength at the regional rather than whole-bone level. Subject-specific finite element analysis (FEA) provides such an approach by integrating individual bone geometry, density, and mechanical response to loading, offering more accurate fracture prediction than BMD or geometry alone [2]. While FEA has been applied regionally, such as in tibial plateau simulations and midshaft strain studies, comprehensive, subject-specific modeling across proximal, midshaft, and distal tibial regions in healthy female athletes is largely absent [3, 4]. To address this gap, we developed a CT-based, individualized FEA workflow to evaluate regional tibial strength and failure risk in female athletes. Using calibrated CT scans, we established a workflow to characterize previously reported loading conditions and analyzed stiffness and stress across the proximal, midshaft, and distal tibia.

METHODS: Participants provided written informed consent, and all procedures were approved by the institutional review board. Two female athletes (23.5 ± 0.7 years; 167.8 ± 5.3 cm; 60.9 ± 3.4 kg) were analyzed as part of a larger dataset of 23 participants. The study workflow is illustrated in Figure 1. CT scans of the left lower leg were obtained using an Optima CT660 (GE Medical Systems) with 120 kVp, 160 mAs, 0.625 mm slice thickness, 0.5 x 0.5 in-plane resolution, and a hydroxyapatite calibration phantom. Tibias were segmented semi-automatically in Materialise MIMICS (v 24.0), and orientation was standardized by vertically aligning tibias in the sagittal plane. CT values were calibrated using the phantom's known densities. Regional FE models were generated from 10 mm image stacks at the proximal third, midshaft, and distal third of the tibia using 10-node tetrahedral elements. Mesh convergence was verified for stiffness and maximum von Mises stress. Each element was assigned CT-derived, density-based isotropic elastoplastic material properties (Poisson's ratio = 0.30), with elastic modulus mapped from calibrated HU values and yield stresses defined using bilinear isotropic plasticity in ANSYS Mechanical (version 2025 R1). To simulate compressive loading, the distal end of the slices was fixed, and 1% axial strain was applied proximally. Simulations estimated tibial stiffness and peak stress.

RESULTS: Finite element analysis of the proximal, midshaft, and distal tibial regions revealed distinct regional mechanical behaviors. Mechanical responses observed were higher than prior reports [2, 3], likely due to slice thickness and subject differences. In our highly fit participants, tibia stiffness was higher in the proximal (684.9 - 726.8 kN/mm) and midshaft (700.9 - 743.8 kN/mm) regions when compared to the distal region (570.4 - 607.1 kN/mm). Similarly, maximum von Mises stress generally tended to be lower proximally (235.8 - 255.5 MPa) and at the midshaft (224.9- 282.3 MPa) than at the distal tibia (233.3 - 251.0 MPa). Correspondingly, mean cortical thickness was greatest at the midshaft (6.0 mm), moderate proximally (5.6 mm), and lowest distally (5.1 mm), supporting the observed regional variation in stiffness and load distribution and aligning with the tibial cross-sectional geometry reported [5].

DISCUSSION: The proximal and midshaft outperformed the distal tibia in both stiffness and stress. For these two participants, the proximal and mid tibia showed greater stiffness and lower internal stress, reflecting its structural optimization for high mechanical loads and thicker cortical bone. In contrast, the distal tibia presented with lower stiffness and higher stress, reflecting its mechanical vulnerability and aligning with its higher injury incidence in athletes. These preliminary findings suggest that the distal region may be less equipped to handle repeated high-impact loading, likely due to thinner cortical bone and less efficient load distribution, making it a priority for injury prevention. These insights may support the need for regionally targeted assessments of bone strength and personalized approaches to reducing injury risk in female athletes. Further research is needed to fully assess the utility of the cross-sectional FEA approach for BSI management. Simple loading was applied here, which may limit the broad real-world application of the simulations. Multi-axial and muscle-driven loading produce strain distributions more reflective of in vivo conditions and would strengthen this model.

SIGNIFICANCE/CLINICAL RELEVANCE: This study highlights the importance of region-specific biomechanical analysis for understanding BSI among female athletes. Traditional whole-bone measures may obscure critical site-specific weaknesses. Combining FEA with clinical imaging tools like pQCT, MRI, and CT could broaden accessibility in orthopedic biomechanics and improve translation. Subject-specific FEA further enables identification of mechanical vulnerabilities, enabling personalized, precision-based strategies for injury prevention, rehabilitation, and return to sport.

[1] Hollander, K, et al. Sports Medicine 51.5 (2021): 1011-1039.
[2] Robinson, DL., et al. Biomechanics and Modeling in Mechanobiology 18.1 (2019): 245-260.
[3] Knowles, N K., et al. Annals of Biomedical Engineering 49.9 (2021): 2389-2398.
[4] Besa, Pablo, et al. Frontiers in Bioengineering and Biotechnology 13 (2025): 1541536.
[5] Franklyn, M, et al. The American journal of sports medicine 36.6 (2008): 1179-1189.

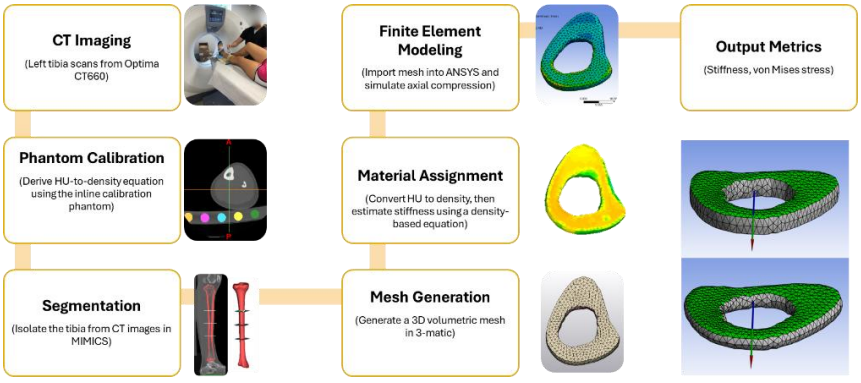

Figure 1. Study workflow from imaging to simulation outcomes